

# Compact “diode-based” multi-energy soft x-ray diagnostic for NSTX<sup>a)</sup>

K. Tritz, D. J. Clayton, D. Stutman, and M. Finkenthal<sup>b)</sup>*The Johns Hopkins University, Baltimore, Maryland 21218, USA*

(Presented 7 May 2012; received 4 May 2012; accepted 3 June 2012; published online 6 July 2012)

A novel and compact, diode-based, multi-energy soft x-ray (ME-SXR) diagnostic has been developed for the National Spherical Tokamak Experiment. The new edge ME-SXR system tested on NSTX consists of a set of vertically stacked diode arrays, each viewing the plasma tangentially through independent pinholes and filters providing an overlapping view of the plasma midplane which allows simultaneous SXR measurements with coarse sub-sampling of the x-ray spectrum. Using computed x-ray spectral emission data, combinations of filters can provide fast ( $>10$  kHz) measurements of changes in the electron temperature and density profiles providing a method to “fill-in” the gaps of the multi-point Thomson scattering system. © 2012 American Institute of Physics. [<http://dx.doi.org/10.1063/1.4731741>]

## I. INTRODUCTION

A novel and compact, diode-based, multi-energy soft x-ray (ME-SXR) diagnostic has been developed for the National Spherical Tokamak Experiment (NSTX).<sup>1</sup> The new diode-based system provides several advantages over the prior “optical array” implementation<sup>2</sup> including increased dynamic range, higher sensitivity and signal-to-noise ratio (SNR) at low energy, calibration stability, and importantly, capability for in-vessel operation. These factors enable SXR detection at lower energy and extend the ME-SXR measurement from the plasma core to the lower temperature edge region. The compact ME-SXR design is also well suited to in-vessel deployment, increasing the flexibility for placement and plasma coverage.

The new edge ME-SXR system tested on NSTX consists of a set of vertically stacked diode arrays, each viewing the plasma tangentially through independent pinholes and filters. The independent pinholes provide an overlapping view of the plasma midplane which allows simultaneous SXR measurements with coarse sub-sampling of the x-ray spectrum provided by the varying cutoff energy thresholds of the different filters. The 5 “energies” used in the present system include a bolometric measurement to constrain radiated power, thin foil filters to detect SXR impurity line emission, and thicker filters to provide continuum measurements.

The primary purpose of the ME-SXR diagnostic is to use the filtered x-ray spectral information to extract electron temperature ( $T_e$ ), density ( $n_e$ ), and impurity information from the SXR measurements. Due to the nature of a low-aspect ratio tokamak plasma, standard high time and spatial resolution imaging of electron temperature using ECE measurements fail as the plasma is over-dense to the emission. However, using computed x-ray spectral emission data, combinations of filters can provide fast ( $>10$  kHz) measurements of

changes in the electron temperature and density profiles providing a method to “fill-in” the gaps of the multi-point Thomson scattering system (MPTS) which operates at 60 Hz on NSTX. The fast ME-SXR profile data can then be used to measure edge localized modes (ELMs) and their effects on the plasma profiles, cold pulse data for perturbative thermal transport measurements, and emission from neon gas or other impurity injections for impurity transport measurements. The ME-SXR measures x-ray line and continuum emission from the plasma with photon energies of 10’s of eV up to  $\sim 10$  keV; therefore, SNR will depend strongly on electron density, temperature, and impurities. The typical plasma parameters for good profile measurements are  $n_e > \text{few } 10^{18} \text{ m}^{-3}$  and  $T_e > \sim 100$  eV depending on the selected filters. The ME-SXR system also complements the existing poloidal ultra-soft x-ray array (USXR) on NSTX, which has a faster measurement bandwidth ( $\sim 200$  kHz) and high sensitivity large area detectors with coarser spatial resolution, 2–4 cm.<sup>3</sup>

## II. HARDWARE

One of the primary design goals of the diode-based ME-SXR system was a compact, modular system to enable maximum flexibility for diagnostic placement and field-of-view (FOV). The detector hardware is shown in Figure 1. The in-vacuum hardware (Fig. 1(a)) is mounted on a 6” conflat flange modified to include 5 D-sub DB25 vacuum electrical feedthroughs. A custom printed circuit board (PCB), composed of the Rogers 3003 vacuum compatible laminate, was designed to mount directly onto each DB25 connection and accept the AXUV-20 20-element diode array from Opto Diode Corp. (formerly International Radiation Detectors Inc.). Each diode array has twenty 0.75 mm wide  $\times$  4 mm high elements sharing a common anode, with a near theoretical response across a wide range of photon energies. Each array is optically isolated to prevent crosstalk, and views the plasma through a separate pinhole and filter combination providing an overlapping FOV of the same plasma volume.

The 1st stage pre-amplifier electronics were mounted directly on the air-side of the DB25 vacuum electrical feedthrough to minimize noise and pickup (Fig. 1(b)). The

<sup>a)</sup>Contributed paper, published as part of the Proceedings of the 19th Topical Conference on High-Temperature Plasma Diagnostics, Monterey, California, May 2012.

<sup>b)</sup>Author to whom correspondence should be addressed. Electronic mail: [ktritz@pppl.gov](mailto:ktritz@pppl.gov).

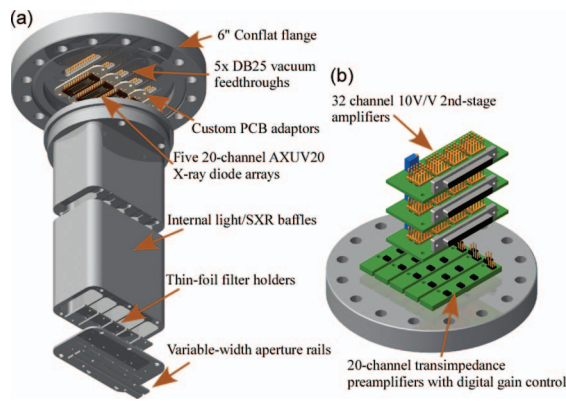


FIG. 1. Exploded view of (a) ME-SXR vacuum hardware and (b) 1st and 2nd stage amplifier electronics.

pre-amplifiers were custom designed circuits based off the MAZeT MTI04 multi-channel, variable gain transimpedance amplifier IC. The output of the 1st stage pre-amplifiers were routed to  $3 \times 32$  channel 2nd stage 10 V/V voltage amplifier circuits with low output impedance capable of driving the cabling used to deliver the ME-SXR signals to the data acquisition system. The built-in variable gains of the MAZeT IC can be manually set using toggle switches or controlled via digital programming using the data acquisition system. The bandwidth and gain can be set from  $2 \times 10^8$  with a corresponding bandwidth of 6 kHz at the highest setting to a gain of  $2.5 \times 10^5$  with a bandwidth of 300 kHz at the lowest. The output of the ME-SXR amplifiers is then sent over 3 50 ft. long HD68 twisted pair cables to the inputs of a DTacq ACQ196CPCI-96-500 data acquisition module which supports 96 simultaneous channels of 16-bit analog-to-digital conversion with a 500 kHz sampling rate and a  $\pm 10$  V full scale input range (Figure 2(b)). The DTacq module also contains 32 channels of digital input/output which is connected directly to the ME-SXR power and control chassis. The ME-SXR power and control module uses a low noise linear regulated power supply to provide clean power to the ME-SXR system along with a negative voltage bias for the AXUV diode arrays. The power and bias along with the digital control signals are bundled into a DB25 cable which connects to the ME-SXR assembly mounted on the machine.

While the shielded twisted pair cabling helps protect the ME-SXR from electrostatic pickup, the challenging electrical environment, and the lack of further signal conditioning adds  $\sim 3$  mV rms of noise to the final digitized signals, allowing a maximum SNR of 6000:1. However, much of this pickup oc-

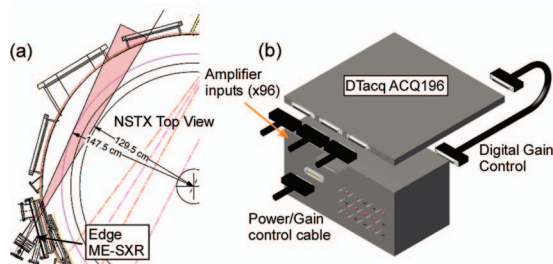


FIG. 2. Schematic of (a) ME-SXR position and FOV on NSTX and (b) DAQ and control electronics for the ME-SXR system.

cur at frequencies much higher than the working bandwidth of the ME-SXR amplifiers, thus digital filtering of the signal can reduce the noise to  $\sim 1.5$  mV rms within the frequency range of interest  $< 100$  kHz.

### III. INITIAL DATA

The ME-SXR was installed on NSTX to provide a high resolution view of the edge plasma with 1 cm resolution with a FOV covering a tangential radius,  $r_{\text{tan}}$  from  $\sim 130$  cm to 148 cm (Figure 2(a)). This edge view was chosen for the study of edge impurity transport,<sup>4</sup> ELM activity, and edge MHD, and other phenomena.

An example of edge phenomena include changes in the edge SXR profile on time and space scales of a few ms and 1–2 cm, respectively, which immediately precede sudden drops in the global plasma profiles. This precursor detail is challenging to measure with conventional profile diagnostics like MPTS (Ref. 5) and charge exchange spectroscopy (CHERS) (Ref. 6) due to the coarse time resolution of those measurements (16 ms and 10 ms, respectively). While hints of this change in the edge SXR emission has been previously observed in the USXR system, the poloidal FOV and coarser spatial resolution had prevented an accurate, high spatial resolution mid-plane reconstruction of the soft x-ray profile. However, the new ME-SXR system can now resolve these events in detail as shown in Figure 3, which illustrates a sudden change in the SXR profile, measured using a  $5 \mu\text{m}$  beryllium filter, in the presence of internal MHD activity. The profile shows an increase of the SXR edge gradient in the region  $\sim 140$  cm and a corresponding flattening at  $\sim 137$  cm. Throughout this process, a coherent 16 kHz MHD mode exists across the measurement region. The MHD at the edge region then slows dramatically, leading up to a global profile crash over the entire measurement domain and a termination of the coherent internal MHD activity.

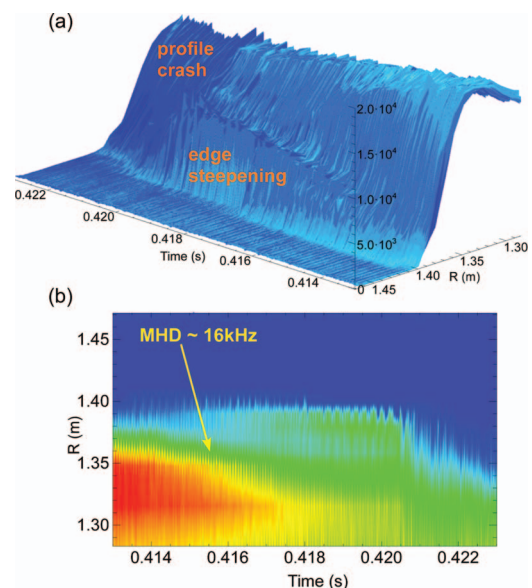


FIG. 3. Plots showing (a) build up of edge SXR emission and (b) internal MHD activity.

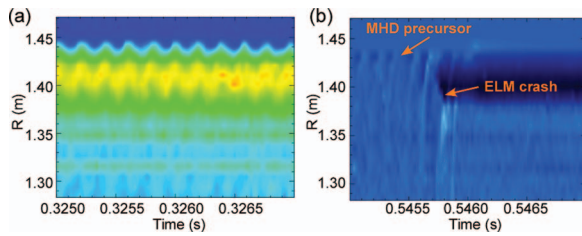


FIG. 4. 5  $\mu\text{m}$  beryllium filtered SXR emission showing (a) small-scale  $\sim 2$  cm 6 kHz edge MHD activity and (b) edge MHD precursor leading to ELM event.

Other, high resolution edge phenomena observed with the initial ME-SXR on NSTX include imaging of small  $\sim 2$  cm, coherent MHD structures (Fig. 4(a)) and ELM activity including small  $\sim 1$  cm MHD edge precursors and the fast ( $\sim 10$  kHz) measurements of the ELM crash dynamics (Fig. 4(b)). These initial measurements demonstrate the type of new high time and space resolved data that will provide important information for the study of edge stability on NSTX.

#### IV. FAST $T_e$ ANALYSIS DESCRIPTION

While the initial ME-SXR data have already provided new and unique measurements of the dynamics of the NSTX edge plasma, the primary goal of the ME-SXR system, as discussed previously, is to provide separate, fast  $T_e$  and  $n_e$  profile measurements and additional information on the impurity content using a similar method to previous work.<sup>7</sup> An in-depth discussion of the detailed algorithms and improvements to the previous method is beyond the scope of this work and will be published in a later article. However, the basic method for disentangling the  $T_e$ ,  $n_e$ , and  $n_z$  contributions to the SXR measurement relies on viewing the same plasma volume through different x-ray filters. The detected SXR emission is related to  $n_e$ ,  $T_e$ , and  $n_z$  as

$$E_f = n_e \sum_Z n_{z,i} R_{f,i}(T_e) = n_e^2 \sum_Z c_i R_{f,i}(T_e), \quad (1)$$

where  $E_f$  is the measured, filtered SXR emission,  $c_i$  is the concentration of ion species “ $i$ ” and  $R_{f,i}$  is the density normalized and filtered radiated emission of the impurity which is predominantly a function of  $T_e$  in the typical range of plasma conditions.  $R_{f,i}$  is calculated from atomic spectral codes, such as ADAS (Ref. 8) which then allows one to assemble a set of equations using the filtered measurements to solve for the unknown  $T_e$ ,  $n_e$ , and impurity concentrations. Snapshots of the  $T_e$  and  $n_e$  profiles provided by MPTS provide additional constraints on the fits and also allow the equations to be recast into a linearized and normalized form (Eq. (2)) which is used to calculate the *change* in  $T_e$  and  $n_e$  from previously measured profiles. This ability to “fill-in” the gaps between MPTS measurements can leverage the increased time resolution of the ME-SXR system while maintaining accuracy by periodically using MPTS as a profile reference. Furthermore, impurity concentrations for carbon, the primary impurity, are provided by the CHERS system, with additional spectroscopy such as the transmission grating imaging spectrometer<sup>9</sup> providing constraints for other ion concentrations. Due to oper-

ational constraints of the new diode-based ME-SXR system, the full system was not available for  $T_e$  reconstruction measurements; however, fast  $T_e$  profiles filling in between MPTS measurements using the previous multi-energy system was demonstrated in a previous work<sup>7</sup>

$$\frac{\Delta E_f}{E_f} = \frac{2\Delta n_e}{n_e} + \frac{\sum_i c_i R'_{f,i}}{\sum_i c_i R_{f,i}} \Delta T_e. \quad (2)$$

#### V. FUTURE WORK

Due to the truncated 2011 NSTX run, the ME-SXR system has accumulated only a few weeks of operational time at partial capacity. However, in that limited time, significant and interesting phenomena have already been observed. In the future, port constraints for the new NSTX-U have motivated a re-entrant redesign of the system to operate within the vacuum vessel chamber, and a fully operational system including both a high resolution edge array and a full-radius core array is expected to be ready for day 1 of NSTX-U operations.

Finally, an “ultra-fast” dual energy system is under development and testing for possible replacement of the present poloidal USXR system on NSTX. The specifications of this system include measurements up to 4 MHz with simultaneous views through dual filters/pinholes. The purpose of this proposed system would be to extricate the temperature and density fluctuations associated with high frequency core Alfvén eigenmodes (AE) on NSTX in an attempt to classify the AEs and investigate their effects on transport.<sup>10,11</sup>

#### ACKNOWLEDGMENTS

The author would like to thank the NSTX team for their assistance and support with work carried out at the Princeton Plasma Physics Laboratory. This work is supported by the Department of Energy Grant Nos. DE-AC02-09CH11466 and DE-FG02-86ER53214.

<sup>1</sup>M. Ono *et al.*, *Nucl. Fusion* **40**(3Y), 557 (2000).

<sup>2</sup>L. F. Delgado-Aparicio, D. Stutman, K. Tritz, M. Finkenthal, R. Kaita, L. Roquemore, D. Johnson, and R. Majeski, *Rev. Sci. Instrum.* **75**, 4020 (2004).

<sup>3</sup>D. Stutman, M. Iovea, M. Finkenthal, R. Kaita, D. Johnson, L. Roquemore, and P. Roney, *Rev. Sci. Instrum.* **72**, 731 (2001).

<sup>4</sup>D. J. Clayton, D. Stutman, K. Tritz, M. Finkenthal, D. Kumar, B. P. LeBlanc, S. Paul, and S. A. Sabbagh, “Multi-energy SXR technique for impurity transport measurements in the fusion plasma edge,” *Plasma Phys. Controlled Fusion* (submitted).

<sup>5</sup>B. P. LeBlanc, R. E. Bell, D. W. Johnson, D. E. Hoffman, D. C. Long, and R. W. Palladino, *Rev. Sci. Instrum.* **74**, 1659 (2003).

<sup>6</sup>R. E. Bell, *Rev. Sci. Instrum.* **77**, 10E902 (2008).

<sup>7</sup>L. F. Delgado-Aparicio, D. Stutman, K. Tritz, M. Finkenthal, R. E. Bell, J. Hosea, R. Kaita, B. LeBlanc, L. Roquemore, and J. R. Wilson, *J. Appl. Phys.* **102**, 073304 (2007).

<sup>8</sup>H. P. Summers, The ADAS User Manual, version 2.6, 2004, see <http://www.adas.ac.uk>.

<sup>9</sup>D. Kumar, D. Stutman, K. Tritz, M. Finkenthal, C. Tarrío, and S. Grantham, *Rev. Sci. Instrum.* **81**, 10E507 (2010).

<sup>10</sup>D. Stutman, L. Delgado-Aparicio, N. Gorelenkov, M. Finkenthal, E. Fredrickson, S. Kaye, E. Mazzucato, and K. Tritz, *Phys. Rev. Lett.* **102**, 115002 (2009).

<sup>11</sup>N. A. Crocker, W. A. Peebles, S. Kubota, J. Zhang, R. E. Bell, E. D. Fredrickson, N. N. Gorelenkov, B. P. LeBlanc, J. E. Menard, M. Podestà, S. A. Sabbagh, K. Tritz, and H. Yuh, *Plasma Phys. Control. Fusion* **53**, 105001 (2011).